



PICK-OBJECT-ATTACK: Type-Specific Adversarial Attack for Object Detection

Omid Mohamad Nezami^{a,2}, Akshay Chaturvedi^{b,2}, Mark Dras^a, Utpal Garain^b

^aMacquarie University, Sydney, NSW, Australia

^bIndian Statistical Institute, Kolkata, India

ABSTRACT

Many recent studies have shown that deep neural models are vulnerable to adversarial samples: images with imperceptible perturbations, for example, can fool image classifiers. In this paper, we present the first type-specific approach to generating adversarial examples for object detection, which entails detecting bounding boxes around multiple objects present in the image and classifying them at the same time, making it a harder task than against image classification. We specifically aim to attack the widely used Faster R-CNN by changing the predicted label for a particular object in an image: where prior work has targeted one specific object (a stop sign), we generalise to arbitrary objects, with the key challenge being the need to change the labels of *all* bounding boxes for all instances of that object type. To do so, we propose a novel method, named PICK-OBJECT-ATTACK. PICK-OBJECT-ATTACK successfully adds perturbations only to bounding boxes for the targeted object, preserving the labels of other detected objects in the image. In terms of perceptibility, the perturbations induced by the method are very small. Furthermore, for the first time, we examine the effect of adversarial attacks on object detection in terms of a downstream task, image captioning; we show that where a method that can modify all object types leads to very obvious changes in captions, the changes from our constrained attack are much less apparent.

© 2021 Elsevier Ltd. All rights reserved.

1. Introduction

Deep learning systems have achieved remarkable success for several computer vision tasks. However, adversarial attacks have brought into question the robustness of such systems. Goodfellow et al. (2014) and Szegedy et al. (2014) presented early attacks against image classifiers, using gradient-based techniques to construct inputs with the ability to fool deep learning systems. Since then adversarial attacks have been extensively studied for image classification, including being shown to be transferable across different image classifiers (Liu et al., 2017). This presents risks for many applications of image processing, such as in forensics or biometrics;³ for example,

Caldelli et al. (2019) present a collection of work on image and video forensics, such as locating splicing forgeries in images (tampered areas of synthesized images) (Liu and Pun, 2018) or detecting image inpainting (Zhu et al., 2018). Adversarial attacks against images are usually categorised into two types (i) Targeted and (ii) Non-targeted. In a targeted attack, the goal is to modify the input so as to make the deep learning system predict a specific class, whereas in a non-targeted attack, the input is modified so as to cause the prediction of any incorrect class.

A more challenging task is to construct adversarial examples that will fool an object detection system, with each image containing multiple objects and multiple proposals for each object; Xie et al. (2017) provide an analysis of this complexity. Chen et al. (2018b) motivate this task with the example of object detection by an autonomous vehicle to recognise a stop sign and the risks involved in an adversarial attack in that context.

These two works tackle the issue of adversarial attacks against object detection and are the most relevant to our work. Xie et al. (2017) propose a non-targeted attack where the predictions of all objects are changed simultaneously. Chen et al. (2018b) propose an attack against the object detector to mis-

^{**}Corresponding author

e-mail: omid.mohamad-nezami@hdr.mq.edu.au (Omid Mohamad Nezami)

²The authors contributed equally to this work.

³There is in fact a contemporaneous special issue of this journal on this topic (Chellappa et al., 2021).

© 2021. This manuscript version is made available under the CC-BY-NC-ND 4.0 license <https://creativecommons.org/licenses/by-nc-nd/4.0/>

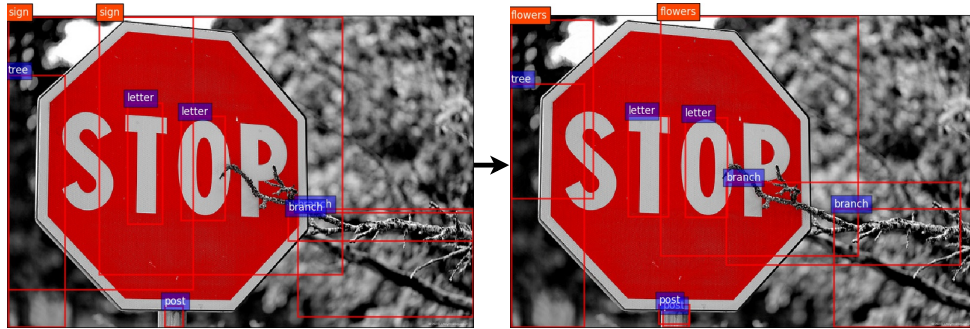


Fig. 1. Example of our adversarial attack. PICK-OBJECT-ATTACK adds imperceptible perturbations to the first image (on the left) resulting in the second image (on the right). It succeeds in changing the predicted class of the targeted object from “sign” to “flowers” (shown in orange) while other predicted classes (shown in blue) are unchanged.

classify only stop sign images; the attack method deliberately adds perceptible noise to the images.

In this paper, the proposed PICK-OBJECT-ATTACK aims to change the label of a particular object while keeping the labels of other detected objects unchanged. In this sense, it is a generalisation of Chen et al. (2018b), where there may be a particular object that the attacker wants to be misclassified. More generally, it is often a goal of adversarial attacks to be imperceptible to observers; attacking just a single object, with the small number of bounding boxes involved, minimises the changes to the image relative to modifying all the objects as in Xie et al. (2017). Moreover, changes to the image — even if imperceptible to humans — could be perceptible via downstream tasks. For instance, object detection plays a crucial role in the state-of-the-art visual question answering (VQA) and image captioning systems (Anderson et al., 2018). Changing the entire image may lead to dramatically different answers or captions and hence alert the user indirectly. Figure 1 shows an example of our proposed PICK-OBJECT-ATTACK. From the figure, we can see that only the label of object type “sign” has changed to “flowers” whereas other objects are detected correctly. This is because the perturbation is only added to the bounding boxes with the predicted label “sign”. Analysing perceptibility of this attack both by standard metrics and via a downstream task contributes to the understanding of risks for forensics.

In this paper, we propose both targeted and non-targeted versions of PICK-OBJECT-ATTACK against Faster R-CNN (Ren et al., 2015), a widely used and high-performing object detector, which Chen et al. (2018b) and Xie et al. (2017) also based their work on. Where they studied a version of Faster R-CNN trained on the MSCOCO dataset (Lin et al., 2014), we use a different Faster R-CNN trained on the Visual Genome dataset (Krishna et al., 2017), covering a larger set of classes than the MSCOCO dataset. Bottom-up features obtained from this version of Faster R-CNN have been employed in state-of-the-art VQA and image captioning systems (Anderson et al., 2018). These systems use the bottom-up and top-down attention to attend to the bounding boxes in order to generate a caption (or answer).

The main contributions of this paper are as follows ⁴:

- I This is the first study to successfully apply both targeted and non-targeted attacks against Faster R-CNN on different types of images. Xie et al. (2017) only study the non-targeted attack against Faster R-CNN and Chen et al. (2018b) only attack stop sign images. The proposed attack achieves high success rates for both targeted ($> 75\%$) and non-targeted ($> 95\%$) attacks. We show that the proposed attack adds imperceptible perturbation to the image. Furthermore, the perturbation is only added to the pixels within a specified object type.
- II This is the first work which studies an adversarial attack against Faster R-CNN in a constrained setting where the label of a particular object in an image is changed while preserving the labels of other detected objects which are outside of the region of interest. We propose an attack which works for arbitrary images and can be straightforwardly generalised to change the labels of multiple detected objects.
- III This is the first work to use a downstream task to contribute to an understanding of perceptibility of adversarial attacks. Specifically, we study the effect of attacking Faster R-CNN on the state-of-the-art image captioning system (Anderson et al., 2018) which uses bottom-up features. We show that it leads to many fewer changes in captions than a method based on Xie et al. (2017) which modifies all the objects.

2. Related work

The generation of adversarial samples was first investigated in the context of deep learning by Szegedy et al. (2014), who used a gradient-based optimization to arbitrarily manipulate the input sample of a deep neural network for image classification. This manipulation usually aims to find similar samples with differences that are imperceptible to human observers, in order to change the predicted class. Later works (Nguyen et al., 2015; Carlini and Wagner, 2017; Eykholt and Prakash, 2018) have led to better methods for generating adversarial samples, via different attack mechanisms, to mislead different classification models. In addition to classification, adversarial samples have also been crafted for other tasks such as image captioning (Chen et al., 2018a; Ji et al., 2020) and visual question answering (Chaturvedi and Garain, 2020). They studied earlier image captioning models (Vinyals et al., 2015; Xu et al., 2015) which use features from image classifiers.

However, in many scenarios including the physical world, we usually face multiple objects in an image. Under such a

⁴Our source code is publicly available at the following link:

<https://github.com/omidmnezami/pick-object-attack>

condition, an attack would be required to fool an object detector, which detects the bounding boxes of objects in addition to classifying them. Eykholt et al. (2018) discussed how misleading an object detector, such as YOLO (Redmon and Farhadi, 2017) and Faster R-CNN (Ren et al., 2015), is more difficult than misleading an image classifier.

In this paper, we propose a white-box attack against Faster R-CNN, which is a highly-cited and high-performing system for object detection. It has been recently used for different important purposes such as object tracking and segmentation (Wang et al., 2019; Chen et al., 2019), image captioning and visual question answering (Anderson et al., 2018; Gao et al., 2019) and so forth. Faster R-CNN consists of two stages, a region proposal network (RPN) for detecting the bounding boxes of objects, and a classifier for classifying the boxes (Ren et al., 2015). Although the RPN can generate a dynamic number of bounding boxes from the image, an upper bound is usually set on the number of bounding boxes ranked by their confidence levels. The confidence level of each bounding box is calculated using the objectness score and non-maximum suppression (NMS). The RPN predicts an objectness score indicating the probability of an object being present inside the box and the NMS threshold reduces the number of detected boxes. The output of Faster R-CNN will be the classification for the detected boxes.

Xu et al. (2020) analysed several popular attacks against object detection models including Faster R-CNN and YOLO. Chen et al. (2018b) proposed both *targeted* and *non-targeted* attacks on Faster R-CNN but only for stop sign images. They selected stop signs due to security-related issues in the real world, e.g. self-driving cars. They added *perceptible* perturbations to make their adversarial samples robust after printing. Very recently, Huang et al. (2019) targeted stop signs, but by adding *perceptible* perturbations around the border of the signs. In contrast, we target a random set of different objects for both *targeted* and *non-targeted* attacks. We add *imperceptible* perturbations to fool Faster R-CNN. Xie et al. (2017) proposed a *non-targeted* attack (DAG) on Faster R-CNN. They added *imperceptible* perturbations to *all pixels* in the input image to change the classes for all detected objects. Here, for the adversarial image, the RPN usually generates a different set of bounding boxes, with different scales. The bounding boxes change because adding the perturbations can change their confidence levels. They also changed the upper bound of detected boxes from 300 to 3000, guaranteeing the transfer of classification error among nearby boxes. The DAG approach has been applied on the PASCAL VOC dataset containing 21 classes. Wang et al. (2020) also proposed a *non-targeted* attack on Faster R-CNN and compared against the DAG approach. However, they only used 256 proposals rather than original 3000 ones in Xie et al. (2017) and did their experiment on Pascal VOC dataset. The notion of success cases in their work is different from Xie et al. (2017). They considered their attacks successful where either the labels or the location of original bounding boxes are changed or new bounding boxes are introduced. However, Xie et al. (2017) called an attack successful if none of the original classes is detected. Thus, we compare against the DAG ap-

proach of Xie et al. (2017). In our PICK-OBJECT-ATTACK, we do not increase the upper bound of number of boxes and only add *imperceptible* perturbations to the boxes corresponding to a targeted object to change its predicted class. We do not change the pixel values of other boxes. Unlike Xie et al. (2017) and Wang et al. (2020), we study both *targeted* and *non-targeted* attacks. Concurrent with our work, Chow et al. (2020) proposed a targeted attack in three different settings including object-vanishing, object-fabrication and object-mislabeling. They performed their experiments on Pascal VOC dataset and MSCOCO dataset containing 81 classes. In contrast, we apply our attack on the Visual Genome dataset containing 1600 classes, and as with previous work, our task definition of attacking all instances of a particular object type differs. For the first time, we also examine the impact of our proposed attacks on the state-of-the-art image captioning system (Anderson et al., 2018).

3. Method

3.1. Faster R-CNN Model

We evaluate our attack method against Faster R-CNN with ResNet-101, pre-trained on the ImageNet dataset (Deng et al., 2009), then trained on the object and attribute instances of the Visual Genome dataset. The model leads to the state-of-the-art on different tasks like image captioning and visual question answering (Anderson et al., 2018) in addition to generating a high object detection performance. Previous works (Xie et al., 2017; Chen et al., 2018b) studied attacking Faster R-CNN trained on the MSCOCO dataset (Lin et al., 2014) having only 80 object classes. In comparison, the Visual Genome dataset has 1600 object classes. It includes 3.8M object instances versus 1.5M for MSCOCO. It also contains 2.8M attributes and 2.3M relationships.

3.2. PICK-OBJECT-ATTACK

Let I_{org} denote the original image. Let N be the number of bounding boxes and K be the number of classes. An object detector can be mathematically expressed as a function $f : I_{org} \rightarrow (g, h)$ where $g \in \mathbb{R}^{N \times K}$ denotes the probability distribution for N bounding boxes, and $h \in \mathbb{R}^{N \times 4}$ denotes the predicted coordinates of the bounding boxes. Let o_{pick} denote the selected object to attack and $\mathbf{a} \subseteq \{1, 2, \dots, N\}$ denote the indexes of the boxes with predicted class o_{pick} for the image I_{org} . Faster R-CNN rescales the input image so that the shortest size is 600 pixels. Given the original image I_{org} of shape s , our proposed attack generates an adversarial image I_{adv} of the same shape. For an image I , we denote the rescaled image (with the shortest side being 600) by I' .

Mask Detection. As mentioned before, our proposed attack aims to change the label of a targeted object o_{pick} . To do so, for each attack, we prepare a binary mask denoted by M which has a same shape as I_{org} . M is 1 for bounding boxes with predicted label o_{pick} and is 0 otherwise. We compute M for the original image and keep M fixed during the attack.

For a loss function L and an image I' (obtained by rescaling image I), we obtain $\nabla_{I'} L$ during the *backward pass* given by

$$\nabla_{I'} L = r \nabla_{I'} L \quad (1)$$

where r is the learning rate and $\nabla_{I'}L$ is the gradient of loss L for image I' . We resize the gradient $\nabla_{I'}L$ and apply the mask M according to the following equation

$$\nabla_I L = M \odot \text{rescale}(\nabla_{I'}L, s) \quad (2)$$

where \odot denotes bitwise multiplication. For the proposed attack, we use the final obtained gradient $\nabla_I L$ for updating image I . We explain the loss functions for both the non-targeted and targeted attacks below.

Non-Targeted Attack. Our goal in the non-targeted attack is to generate an image I_{adv} so that none of the detected boxes have the predicted class o_{pick} . To achieve this, we use the following loss function, L given by

$$L = - \sum_{a \in \mathbf{a}} \log(g_{a, o_{pick}}) \quad (3)$$

where $g_{i,j}$ denotes the predicted probability of the j^{th} class for the i^{th} box. The proposed attack modifies the image I , via gradient-ascent, using the gradient, $\nabla_I L$. We have two variants: one attacks the most confident object (o_{pick} is the most confident object) called NON-TAR-CONFIDENT and another one attacks the most frequent object (o_{pick} is the most frequent object) called NON-TAR-FREQUENT. These are the most challenging setups: choosing a low-confidence or less-frequent object would make it easier to induce a misclassification. These attacks run for max_{iter} iterations for a fixed r , and the attack is considered unsuccessful if we fail to achieve the goal.

Targeted Attack. Our goal in the targeted attack is to generate an image I_{adv} so that none of the detected boxes have the predicted class o_{pick} and some of the boxes have the predicted class k . Here, k denotes the targeted class for the selected object o_{pick} . To achieve this, we use the following loss function, L given by

$$L = - \sum_{a \in \mathbf{a}} \log(g_{a,k}) \quad (4)$$

where $g_{i,j}$ denotes the predicted probability of the j^{th} class for the i^{th} box. The proposed attack modifies the image I , via gradient-descent, using the gradient, $\nabla_I L$. Similar to the non-targeted attack, we have two variants: TAR-CONFIDENT and TAR-FREQUENT. These attacks run for max_{iter} iterations for a fixed r , and the attack is considered unsuccessful if our goal is not achieved. During the attack, if there are no boxes with label o_{pick} , we set \mathbf{a} to be the box having the maximum probability of k among all the boxes having a positive Intersection over Union (IoU) with the mask M . We give details of the algorithms in the supplementary material.

4. Evaluation Setup

4.1. Intrinsic Evaluation

Success Rate. We use success rate defined as the percentage of attacks that successfully generate adversarial examples. This is a common metric for evaluating adversarial attacks (higher means better performance).

ACAC and ACTC. We adapt these measures for object detectors from attacks against classifiers (Ling et al., 2019). For the non-targeted attacks, Average Confidence of True Class (ACTC) is calculated for object class o_{pick} for all predicted boxes with positive IoU with the mask. This is a performance metric measuring the success of the attack methods to escape from o_{pick} (lower means better performance). For the targeted attacks, Average Confidence of Adversarial Class (ACAC) is calculated for object class k for all predicted boxes with label k . This shows the confidence of the attack methods to generate k (higher means better performance).

Perceptibility. To quantify the perceptibility of change in image, we follow previous work (Szegedy et al., 2014; Xie et al., 2017) in calculating a score δ for an adversarial perturbation given by

$$\delta_i = \frac{\|I_{i,adv} - I_{i,org}\|_2}{\sum M_i} \quad (5)$$

where $I_{i,adv}$ is the i^{th} adversarial image, $I_{i,org}$ is the i^{th} original image, and M_i is the mask of the i^{th} image in pixels. We normalize the ℓ_2 norm of the image difference by the size of the mask, as our proposed attack adds noise only inside the mask and the size of the mask varies across images (lower means better performance).

The Structural SIMilarity (SSIM). We calculate the Structural Similarity (SSIM) to measure the similarity between the original image and the adversarial example since it is a metric which correlates well with human perception. The definition of $SSIM(I_{org}, I_{adv})$ between a single original image I_{org} and an adversarial sample I_{adv} is given in Wang et al. (2004). We calculate the mean SSIM across all pairs of original and adversarial images (higher means better performance).

mAP. Mean average precision (mAP) is calculated for objects outside the mask M . The high value of mAP signifies that other objects outside the mask were detected correctly. mAP is calculated using original prediction as ground truth (higher means better performance).

Implementation Details. We test our proposed attack on a set of 1000 randomly selected images which belong to both Visual Genome and the validation set of the MSCOCO dataset. For the targeted attacks, we run attacks for 10 randomly chosen objects (k) per image resulting in 10k samples. We fix the learning rate in Equation 1 (r) to 10k and set the maximum of iterations (max_{iter}) to 60. As a comparison to our PICK-OBJECT-ATTACK, we design a non-targeted attack (DAG) against *all* objects based on Xie et al. (2017). We choose a fixed label for all the boxes and do gradient descent until none of the original objects are detected. (We give the algorithm in the supplementary material.) We use the same learning rate as our previous attacks for a fair comparison and increase max_{iter} to 120. Since attacking all objects is a difficult task, we obtained a low success rate for DAG (targeted attack against all objects is not feasible) when max_{iter} was set to 60.

Table 1. Success Rate (SR), ACAC, ACTC and mAP for different proposed attacks.

APPROACHES	SR	ACAC	ACTC	mAP
DAG	79.80%	-	-	0.30%
TAR-FREQUENT	89.90%	26.55%	-	86.09%
TAR-CONFIDENT	76.97%	24.53%	-	91.97%
NON-TAR-FREQUENT	95.30%	-	1.25%	94.20%
NON-TAR-CONFIDENT	98.40%	-	2.59%	95.47%

4.2. Downstream Evaluation

Metrics. The standard image captioning metrics (BLEU (Papineni et al., 2002), METEOR (Denkowski and Lavie, 2014), CIDEr (Vedantam et al., 2015), ROUGE (Lin, 2004) and SPICE (Anderson et al., 2016)) are used to compare generated captions with human-produced reference captions, and higher scores indicate greater overlap with these reference captions. We will use these slightly differently. Here, we are interested in the overlap of the caption for the adversarial image and *the caption for the original image*, used as the reference caption. A higher score means that the two captions are more similar, i.e. the caption for the adversarial image is less distorted. In addition, we calculate the percentage of cases for which the proposed attacks can remove the keyword corresponding to o_{pick} from the adversarial caption when the keyword is present in the original caption (KWR).

Implementation Details. We generate captions using three non-targeted attacks: DAG, NON-TAR-FREQUENT, NON-TAR-CONFIDENT and two targeted attacks: TAR-FREQUENT, TAR-CONFIDENT. To do so, we use 100 successful adversarial examples for the non-targeted attacks for a shared set having 100 images (these images belong to MSCOCO dataset). We use 1000 successful adversarial examples for the targeted attacks for the shared set (10 per image).

5. Results

5.1. Intrinsic Evaluation

Quantitative Results. Table 1 shows the success rate, ACAC and ACTC for DAG and our variants of the PICK-OBJECT-ATTACK. The goal of the DAG algorithm is none of the original objects are detected. This leads to a low success rate. Comparing the variants of the PICK-OBJECT-ATTACK, the non-targeted attacks are more successful compared to the targeted ones. Since we only need to induce a misclassification for the non-targeted attacks, we can achieve a better success rate. TAR-CONFIDENT has the lowest success rate. For TAR-CONFIDENT, out of 2303 unsuccessful attacks, 1750 attacks are unsuccessful only because TAR-CONFIDENT cannot find any bounding box with a positive IoU with the mask. This never happens for TAR-FREQUENT since the mask is larger for the most frequent object in comparison with the most confident one in the image. Out of the cases where there is a bounding box with positive IoU with the mask for TAR-CONFIDENT, the success rate is 93.30%. NON-TAR-CONFIDENT produces the highest success rate since it does not face this condition. The ACAC and ACTC metrics here show that the attack approaches can generate high confidence for adversarial and low confidence for original classes. Note that we

Table 2. Mean and standard deviation of ℓ_2 -norm of the difference image normalised by the image size, and SSIM between original and adversarial images.

APPROACHES	ℓ_2 -norm		SSIM
	MEAN	STD. DEV.	
DAG	1.39×10^{-3}	5.28×10^{-4}	94.33%
TAR-FREQUENT	1.18×10^{-3}	4.20×10^{-4}	98.53%
TAR-CONFIDENT	1.14×10^{-3}	4.19×10^{-4}	98.73%
NON-TAR-FREQUENT	4.93×10^{-4}	2.32×10^{-4}	99.22%
NON-TAR-CONFIDENT	4.07×10^{-4}	2.29×10^{-4}	99.32%

Table 3. Mean and standard deviation, for the successful cases, of δ .

APPROACHES	δ	
	MEAN	STD. DEV.
TAR-FREQUENT	1.53×10^{-3}	1.41×10^{-3}
TAR-CONFIDENT	1.06×10^{-2}	2.82×10^{-2}
NON-TAR-FREQUENT	6.62×10^{-4}	8.97×10^{-4}
NON-TAR-CONFIDENT	6.65×10^{-3}	1.58×10^{-2}

do not report ACAC and ACTC for DAG since there is no notion of adversarial and true class when attacking all the objects. To understand the way in which the perturbations contribute to attack success, following Xie et al. (2017) we also randomly permute the perturbations generated by the proposed attacks for the adversarial images. This leads to near zero success rates for all attacks, showing that the spatial structure of the perturbations plays a major role in fooling Faster R-CNN rather than the magnitude of the perturbations.

Table 1 also shows the mAP metric for DAG and our proposed attacks. DAG adds perturbations to the entire image. Hence, for DAG, we calculate mAP for all detected objects. Table 1 shows that DAG generates very low mAP value owing to its high success rate. On the other hand, the variants of PICK-OBJECT-ATTACK add perturbations only inside the mask with the purpose of preserving the labels of the bounding boxes outside the mask. This perturbation may lead to a different set of bounding boxes by the region proposal network (RPN). These bounding boxes are more likely to have a positive IoU with the mask. Here, mAP shows the impact of perturbation on the bounding boxes outside the mask. As shown in Table 1, the proposed attacks mostly do not change the bounding boxes since they generate high mAP values. These results demonstrate that there are two factors impacting on the mAP: the amount of perturbations and the size of the mask. Our targeted attacks add more perturbations to images in order to fool Faster R-CNN to detect targeted classes, and they have lower values for the mAP in comparison with the non-targeted attacks. The attacks against the most frequent objects (TAR-FREQUENT and NON-TAR-FREQUENT) also generate lower mAP than the most confident objects (TAR-CONFIDENT and NON-TAR-CONFIDENT) since the size of the mask for the frequent objects is larger than the confident objects.

As shown in Table 2, SSIM is high for all attack approaches. This shows that the approaches are successful in adding imperceptible perturbations to images. Although, compared to DAG, our proposed approaches achieve higher SSIM. (We show histograms of the number of boxes/iterations and visualize the perturbations of the adversarial examples in the supplementary material). To compare against DAG, we normalize ℓ_2 -norm by the image size in Table 2. As per the results, the proposed approaches lead to lower ℓ_2 -norm than DAG.

Table 3 shows the mean and standard deviation of δ for *successful* cases. TAR-CONFIDENT generates the highest δ . Similarly, NON-TAR-CONFIDENT has higher δ in comparison with NON-TAR-FREQUENT. This means that attacking the most confident object is harder than attacking the most frequent object in the image, even though there are typically more instances of the most frequent object. In fact, from Table 3, we can see that NON-TAR-CONFIDENT requires more noise than TAR-FREQUENT. In the supplementary material, we also show the robustness of the adversarial images against resizing with different scales.

Qualitative Results. Consider the pair of images in the upper row of Figure 2. For generating the adversarial image on the right, we targeted “cat” for “sheep” in this example. The outputs of Faster R-CNN (the labels of bounding boxes) show that “sheep” is changed to “cat”. Similarly, in the lower row, the targeted attack approach successfully changes all instances of “bird” to “sign” as shown in the labels of bounding boxes. Note that Figure 2 shows only bounding boxes which are fed to the captioning system. Since the captioning system picks the top scoring bounding boxes from Faster R-CNN, we obtain different bounding boxes for the original and the adversarial images.

5.2. Downstream Evaluation

Quantitative Results. Table 4 shows the image captioning metrics for different attack approaches. Since DAG changes the whole image, it generates the lowest values for the metrics. The differences are quite dramatic: BLEU-1 is much smaller for DAG than for any variant of PICK-OBJECT-ATTACK; BLEU-3 is zero for DAG which shows that there are zero overlaps of trigrams (sequences of three words) between perturbed and original captions. Comparing our PICK-OBJECT-ATTACK variants, TAR-FREQUENT and NON-TAR-FREQUENT change more regions in the image because they attack the most frequent object. Thus, they generate lower values in comparison with TAR-CONFIDENT and NON-TAR-CONFIDENT, respectively. The targeted attacks have lower values in comparison with the non-targeted ones since they add more perturbations to images to generate particular classes. From these results, it is evident that fewer changes in the image lead to fewer changes in the corresponding captions.

In terms of keyword removal (KWR), TAR-CONFIDENT and NON-TAR-CONFIDENT have higher values in comparison with TAR-FREQUENT and NON-TAR-FREQUENT since they add more perturbations to change the label of the most confident object in the image. TAR-FREQUENT and TAR-CONFIDENT have higher values than their non-targeted versions since they aim to generate a particular class (since o_{pick} is not fixed for DAG, we do not provide KWR for this approach). To study perceptibility of attack, we calculate mean, standard deviation of ℓ_2 -norm of the difference image and SSIM between the adversarial images, used for the downstream evaluation, and the original images. Since DAG modifies the whole image, to compare across attacks, we normalize the ℓ_2 -norm of the difference image by the image size for all attacks (we include ℓ_2 -norm normalised by mask size, as per Equation 5, in Table 6, for direct comparison with Table 3). As shown in Table 5, all methods generate perturbations with low perceptibility according to the standard metrics for adversarial examples. The non-targeted variants of PICK-OBJECT-

ATTACK are less detectable than the targeted ones; DAG is more similar to the targeted variants of PICK-OBJECT-ATTACK, although the perturbations are still small. The perceptibility of DAG by these standard metrics, however, contrasts strongly with the effects on the downstream image captioning task that we describe above, strongly suggesting that the evaluation of how detectable adversarial perturbations are should extend beyond the standard perceptibility metrics.

Qualitative Results. Figure 2 shows two examples fed into the captioning model (the attention weights of the model for these examples are visualized in the Figures 5 and 6 in the supplementary material). The original image in the first row leads to the caption of “a sheep laying in the grass next to a tree”. As discussed in §5.1, a targeted attack changes “sheep” to “cat”; the caption is correspondingly changed to “a cat is laying down in the grass”. This means that our attack against Faster R-CNN can indirectly attack the captioning model to generate a different caption with our targeted class (“cat”). This is also true for the image in the second row for generating a different caption. The original caption for the image is “a man sitting on a bench with two birds”. As noted in §5.1, the attack approach successfully changes “bird” to “sign”; the caption for the adversarial example here is “a man sitting on a bench with a skateboard” which is different from the original one. Although the attack model leads to a new caption, the caption does not include our targeted class (“sign”); “skateboard” is chosen because it is strongly favoured by the language model. As indicated by Table 4, DAG changes captions much more dramatically. (In the supplementary material, we show some more examples of predicted captions.)

6. Conclusion and Future work

We have proposed PICK-OBJECT-ATTACK, a type-specific adversarial attack for Faster R-CNN. The proposed approach attacks a specific object in an image and aims to preserve the labels of other detected objects in the image. We study both targeted and non-targeted attacks. For each one, we have two variants: attacking the most frequent and the most confident object in the image. Amongst them, the lowest success rate is obtained by the TAR-CONFIDENT because this approach sometimes fails to find bounding boxes within the mask. The results show that attacking the most confident object requires more noise than the most frequent object. The proposed attacks achieve high mAP values for bounding boxes outside the mask which shows that they preserve the labels of other detected objects. The results also show that the variants of PICK-OBJECT-ATTACK lead to less noise in comparison with a baseline attack (DAG) adapted from Xie et al. (2017) that modifies the entire image. In addition to standard perceptibility metrics, we carried out an evaluation on a downstream task, studying the impact of the adversarial images on a state-of-the-art image captioning system. We compared the captions generated by different variants of PICK-OBJECT-ATTACK with DAG. The results show that although all models produce perturbations with low perceptibility, DAG produces dramatically distorted captions, in contrast with PICK-OBJECT-ATTACK, suggesting that evaluation on downstream tasks would be a useful complement to standard perceptibility measures. In the context of applications like forensics, for example,

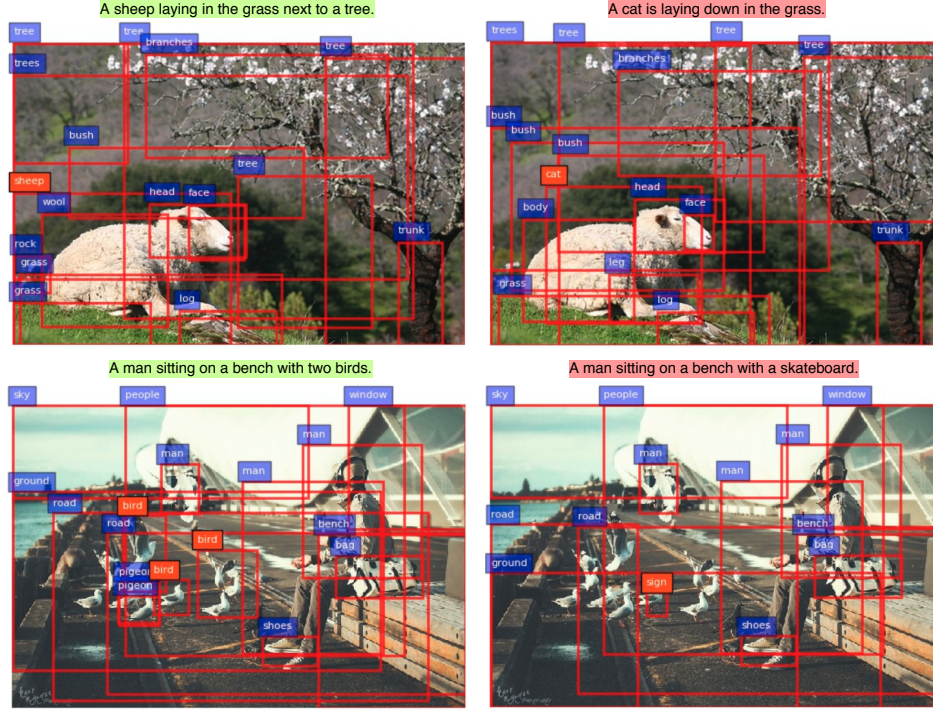


Fig. 2. The first column includes the original images and the second column includes the adversarial images with their corresponding generated captions. The bounding boxes and the labels on these images are the outputs of Faster R-CNN.

Table 4. Image captioning metrics and KWR (in %) for different attacks (B-N is BLEU-N).

APPROACHES	B-1	B-2	B-3	B-4	CIDEr	METEOR	ROUGE-L	SPICE	KWR
DAG	23.15	6.91	0.00	0.00	5.59	8.19	22.70	0.86	-
TAR-FREQUENT	44.77	31.82	24.45	19.58	179.26	20.67	44.03	22.98	72.43
TAR-CONFIDENT	57.73	47.57	40.92	35.81	331.74	30.30	57.28	40.19	80.17
NON-TAR-FREQUENT	63.28	53.23	46.27	40.62	389.55	33.06	62.91	48.16	54.00
NON-TAR-CONFIDENT	70.39	62.59	56.98	52.48	495.17	38.03	69.39	57.18	76.00

Table 5. Mean and standard deviation of ℓ_2 -norm of the difference image normalised by the image size, and SSIM between original and adversarial images for the captioning examples.

APPROACHES	ℓ_2 -norm		SSIM
	MEAN	STD. DEV.	
DAG	1.40×10^{-3}	3.97×10^{-4}	98.23%
TAR-FREQUENT	1.22×10^{-3}	4.86×10^{-4}	98.16%
TAR-CONFIDENT	1.20×10^{-3}	4.61×10^{-4}	98.42%
NON-TAR-FREQUENT	4.55×10^{-4}	2.24×10^{-4}	99.12%
NON-TAR-CONFIDENT	4.08×10^{-4}	2.50×10^{-4}	99.23%

Table 6. Mean and standard deviation of δ for the captioning examples.

APPROACHES	δ	
	MEAN	STD. DEV.
TAR-FREQUENT	1.49×10^{-3}	8.40×10^{-4}
TAR-CONFIDENT	8.37×10^{-3}	1.85×10^{-2}
NON-TAR-FREQUENT	5.52×10^{-4}	3.35×10^{-4}
NON-TAR-CONFIDENT	4.18×10^{-3}	8.39×10^{-3}

this indicates that type-specific adversarial attacks against object detection are harder to detect than broader sorts of attacks.

In future work, we aim to study the more challenging task of attacking attributes as well as objects detected by Faster R-CNN, simultaneously: the challenge here is that it is relatively straightforward for an object detector to learn a set of attributes corresponding to a specific object, and so multiple sources of information have to be perturbed.

References

- Anderson, P., Fernando, B., Johnson, M., Gould, S., 2016. Spice: Semantic propositional image caption evaluation, in: ECCV, Springer. pp. 382–398.
- Anderson, P., He, X., Buehler, C., Teney, D., Johnson, M., Gould, S., Zhang, L., 2018. Bottom-up and top-down attention for image captioning and visual question answering, in: Proceedings of the IEEE conference on computer vision and pattern recognition, pp. 6077–6086.
- Caldelli, R., Chaumont, M., Li, C., Amerini, I., 2019. Special issue on deep learning in image and video forensics. Signal Processing: Image Communication 75, 199–200.
- Carlini, N., Wagner, D., 2017. Towards evaluating the robustness of neural networks, in: 2017 IEEE Symposium on Security and Privacy (SP), IEEE. pp. 39–57.
- Chaturvedi, A., Garain, U., 2020. Attacking vqa systems via adversarial background noise. IEEE Transactions on Emerging Topics in Computational Intelligence 4, 490–499.
- Chellappa, R., Gragnaniello, D., Li, C.T., Marra, F., Singh, R., 2021. Guest Editorial: Adversarial Deep Learning in Biometrics & Forensics. Computer Vision and Image Understanding 208–209, 103227. URL: <https://www.sciencedirect.com/science/article/pii/S1077314221000710>, doi:<https://doi.org/10.1016/j.cviu.2021.103227>.
- Chen, H., Zhang, H., Chen, P.Y., Yi, J., Hsieh, C.J., 2018a. Attacking visual language grounding with adversarial examples: A case study on neural image captioning, in: Proceedings of the 56th Annual Meeting of the Association for Computational Linguistics (Volume 1: Long Papers), pp. 2587–2597.
- Chen, S.T., Cornelius, C., Martin, J., Chau, D.H.P., 2018b. Shapeshifter: Robust physical adversarial attack on faster r-cnn object detector, in: Joint European Conference on Machine Learning and Knowledge Discovery in Databases, Springer. pp. 52–68.
- Chen, X., Girshick, R., He, K., Dollár, P., 2019. Tensormask: A foundation

- for dense object segmentation, in: *Proceedings of the IEEE International Conference on Computer Vision*, pp. 2061–2069.
- Chow, K.H., Liu, L., Gursoy, M.E., Truex, S., Wei, W., Wu, Y., 2020. Understanding object detection through an adversarial lens, in: *European Symposium on Research in Computer Security*, Springer. pp. 460–481.
- Deng, J., Dong, W., Socher, R., Li, L.J., Li, K., Fei-Fei, L., 2009. Imagenet: A large-scale hierarchical image database, in: *2009 IEEE conference on computer vision and pattern recognition*, Ieee. pp. 248–255.
- Denkowski, M., Lavie, A., 2014. Meteor universal: Language specific translation evaluation for any target language, in: *WMT*, pp. 376–380.
- Eykholt, K., Evtimov, I., Fernandes, E., Li, B., Rahmati, A., Xiao, C., Prakash, A., Kohno, T., Song, D., 2018. Robust physical-world attacks on deep learning visual classification, in: *Proceedings of the IEEE Conference on Computer Vision and Pattern Recognition*, pp. 1625–1634.
- Eykholt, K., Prakash, A., 2018. Designing adversarially resilient classifiers using resilient feature engineering. *arXiv preprint arXiv:1812.06626*.
- Gao, P., Jiang, Z., You, H., Lu, P., Hoi, S.C., Wang, X., Li, H., 2019. Dynamic fusion with intra-and inter-modality attention flow for visual question answering, in: *Proceedings of the IEEE Conference on Computer Vision and Pattern Recognition*, pp. 6639–6648.
- Goodfellow, I.J., Shlens, J., Szegedy, C., 2014. Explaining and harnessing adversarial examples. *arXiv preprint arXiv:1412.6572*.
- Huang, Y., Kong, A.W.K., Lam, K.Y., 2019. Attacking object detectors without changing the target object, in: *Pacific Rim International Conference on Artificial Intelligence*, Springer. pp. 3–15.
- Ji, J., Sun, X., Zhou, Y., Ji, R., Chen, F., Liu, J., Tian, Q., 2020. Attacking image captioning towards accuracy-preserving target words removal, in: *Proceedings of the 28th ACM International Conference on Multimedia*, pp. 4226–4234.
- Krishna, R., Zhu, Y., Groth, O., Johnson, J., Hata, K., Kravitz, J., Chen, S., Kalantidis, Y., Li, L.J., Shamma, D.A., et al., 2017. Visual genome: Connecting language and vision using crowdsourced dense image annotations. *International Journal of Computer Vision* 123, 32–73.
- Lin, C.Y., 2004. Rouge: A package for automatic evaluation of summaries. *Text Summarization Branches Out*.
- Lin, T.Y., Maire, M., Belongie, S., Hays, J., Perona, P., Ramanan, D., Dollár, P., Zitnick, C.L., 2014. Microsoft coco: Common objects in context, in: *European conference on computer vision*, Springer. pp. 740–755.
- Ling, X., Ji, S., Zou, J., Wang, J., Wu, C., Li, B., Wang, T., 2019. Deepsec: A uniform platform for security analysis of deep learning model, in: *IEEE S&P*.
- Liu, B., Pun, C.M., 2018. Locating splicing forgery by fully convolutional networks and conditional random field. *Signal Processing: Image Communication* 66, 103–112.
- Liu, Y., Chen, X., Liu, C., Song, D., 2017. Delving into transferable adversarial examples and black-box attacks, in: *Proceedings of 5th International Conference on Learning Representations*.
- Nguyen, A., Yosinski, J., Clune, J., 2015. Deep neural networks are easily fooled: High confidence predictions for unrecognizable images, in: *Proceedings of the IEEE conference on computer vision and pattern recognition*, pp. 427–436.
- Papineni, K., Roukos, S., Ward, T., Zhu, W.J., 2002. Bleu: a method for automatic evaluation of machine translation, in: *ACL, Association for Computational Linguistics*. pp. 311–318.
- Redmon, J., Farhadi, A., 2017. Yolo9000: Better, faster, stronger, in: *The IEEE Conference on Computer Vision and Pattern Recognition (CVPR)*.
- Ren, S., He, K., Girshick, R., Sun, J., 2015. Faster r-cnn: Towards real-time object detection with region proposal networks, in: *Advances in neural information processing systems*, pp. 91–99.
- Szegedy, C., Zaremba, W., Sutskever, I., Bruna, J., Erhan, D., Goodfellow, I., Fergus, R., 2014. Intriguing properties of neural networks, in: *ICLR*.
- Vedantam, R., Lawrence Zitnick, C., Parikh, D., 2015. Cider: Consensus-based image description evaluation, in: *CVPR, IEEE*. pp. 4566–4575.
- Vinyals, O., Toshev, A., Bengio, S., Erhan, D., 2015. Show and tell: A neural image caption generator, in: *Proceedings of the IEEE conference on computer vision and pattern recognition*, pp. 3156–3164.
- Wang, Q., Zhang, L., Bertinetto, L., Hu, W., Torr, P.H., 2019. Fast online object tracking and segmentation: A unifying approach, in: *Proceedings of the IEEE conference on computer vision and pattern recognition*, pp. 1328–1338.
- Wang, Y., Wang, K., Zhu, Z., Wang, F.Y., 2020. Adversarial attacks on faster r-cnn object detector. *Neurocomputing* 382, 87–95.
- Wang, Z., Bovik, A.C., Sheikh, H.R., Simoncelli, E.P., et al., 2004. Image quality assessment: from error visibility to structural similarity. *IEEE transactions on image processing* 13, 600–612.
- Xie, C., Wang, J., Zhang, Z., Zhou, Y., Xie, L., Yuille, A., 2017. Adversarial examples for semantic segmentation and object detection, in: *Proceedings of the IEEE International Conference on Computer Vision*, pp. 1369–1378.
- Xu, B., Zhu, J., Wang, D., 2020. Adversarial attacks for object detection, in: *2020 39th Chinese Control Conference (CCC)*, IEEE. pp. 7281–7287.
- Xu, K., Ba, J., Kiros, R., Cho, K., Courville, A., Salakhudinov, R., Zemel, R., Bengio, Y., 2015. Show, attend and tell: Neural image caption generation with visual attention, in: *International conference on machine learning*, pp. 2048–2057.
- Zhu, X., Qian, Y., Zhao, X., Sun, B., Sun, Y., 2018. A deep learning approach to patch-based image inpainting forensics. *Signal Processing: Image Communication* 67, 90–99.

Supplementary Material

Algorithm 1: NON-TAR-CONFIDENT/ NON-TAR-FREQUENT

Input: $I_{org}, r, max_{iter}, o_{pick}$
Output: I_{adv}
 Get mask M from I_{org} and o_{pick}
 $success \leftarrow \text{False}$
 $I \leftarrow I_{org}$
for $j \leftarrow 1$ **to** max_{iter} **do**
 Compute a for image I
 if $a = \emptyset$ **then**
 $success \leftarrow \text{True}$
 break
 Compute loss L using Equation 3
 Compute $\nabla_I L$ using Equation 2
 $I \leftarrow I + \nabla_I L$
 Truncate image I in the range $[0, 255]$
end for
 $I_{adv} \leftarrow I$
return I_{adv}

Algorithm 2: TAR-CONFIDENT/ TAR-FREQUENT

Input: $I_{org}, r, max_{iter}, o_{pick}, k$
Output: I_{adv}
 Get mask M from I_{org} and o_{pick}
 $success \leftarrow \text{False}$
 $I \leftarrow I_{org}$
for $j \leftarrow 1$ **to** max_{iter} **do**
 Compute a for image I
 if $a = \emptyset$ **then**
 $a = \arg \max_u g_{u,k}$ where u are set of
 predicted boxes with positive IoU with mask M
 if $k = \arg \max_c g_{a,c}$ **for any** $a \in a$ **and**
 $o_{pick} \neq \arg \max_c g_{a,c}$ **for all** $a \in a$ **then**
 $success \leftarrow \text{True}$
 break
 Compute loss L using Equation 4
 Compute $\nabla_I L$ using Equation 2
 $I \leftarrow I - \nabla_I L$
 Truncate image I in the range $[0, 255]$
end for
 $I_{adv} \leftarrow I$
return I_{adv}

7. Scales

Table 7 shows the robustness of adversarial images generated using the proposed attacks against resizing with different scales. The targeted attacks are more robust in comparison with the non-targeted attacks since they add more perturbations to images to generate particular classes. These results show that

Algorithm 3: DAG

Input: I_{org}, r, max_{iter}
Output: I_{adv}
 $c_{org} \leftarrow$ set of predicted classes for I_{org}
 Randomly select class $z \notin c_{org}$
 $success \leftarrow \text{False}$
 $I \leftarrow I_{org}$
for $j \leftarrow 1$ **to** max_{iter} **do**
 if $\arg \max_c g_{b,c} \notin c_{org}$ **for all boxes** b **then**
 $success \leftarrow \text{True}$
 break
 $L \leftarrow -\sum_b \log(g_{b,z})$
 $\nabla_I L \leftarrow \text{rescale}(\nabla'_I L, s)$
 $I \leftarrow I - \nabla_I L$
 Truncate image I in the range $[0, 255]$
end for
 $I_{adv} \leftarrow I$
return I_{adv}

Table 7. Success Rate for our proposed attacks after resizing the adversarial images with different scales: 0.6, 0.8, 1.2 and 1.4.

APPROACHES	Scale			
	0.6	0.8	1.2	1.4
TAR-FREQUENT	16.75%	44.70%	72.35%	78.30%
TAR-CONFIDENT	11.30%	38.08%	65.72%	74.32%
NON-TAR-FREQUENT	2.31%	9.76%	26.76%	34.63%
NON-TAR-CONFIDENT	14.23%	26.42%	42.78%	52.34%

the adversarial images are more robust for bigger scales in comparison with smaller scales.

8. Histograms

Figure 3 shows the histograms of number of boxes and mean probabilities. The first row includes the histogram of the number of boxes, having the predicted label as the targeted class (k), with a positive IoU with the mask. It also includes the histogram of the mean probabilities of the targeted class for the boxes in the targeted attacks. The second row includes the histogram of the number of boxes with a positive IoU with the mask. It also includes the histogram of mean probabilities of the original class (o_{pick}) for the boxes in the non-targeted attacks. This confirms that as expected the total number of boxes for the frequent object is greater than the confident object. The mean probability of the targeted class for both TAR-CONFIDENT and TAR-FREQUENT are almost similar; however, the mean probability of the original class for NON-TAR-CONFIDENT is more than NON-TAR-FREQUENT.

Figure 4 shows the histogram of number of iterations. The first row shows the histogram of the number of iterations for the targeted attacks and the second row for the non-targeted attacks. The maximum number of iterations is 60. If an attack takes 60 iterations, this indicates an unsuccessful attack (we do not show the unsuccessful attacks for TAR-CONFIDENT when

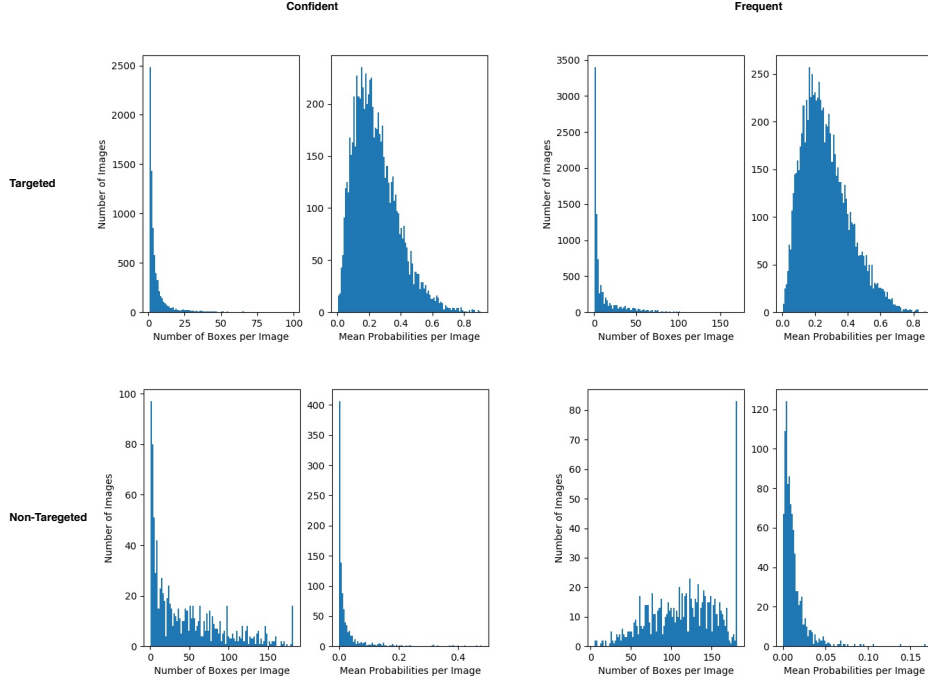


Fig. 3. The histograms of number of boxes and mean probabilities for different variants of PICK-OBJECT-ATTACK.

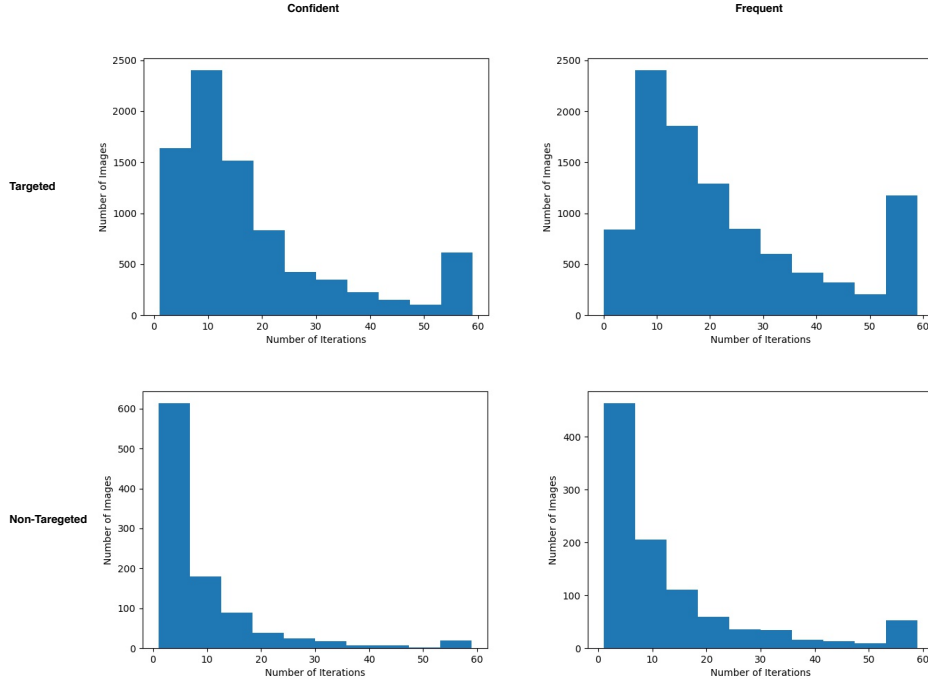


Fig. 4. The histogram of number of iterations for different variants of PICK-OBJECT-ATTACK.

there is no bounding box having a positive IoU with the mask). The histograms show that attacking the most frequent object requires more iterations in comparison with attacking the most confident object. This is because attacking the most frequent object requires changing the label of more boxes in the image. As expected, the targeted attacks take more iterations than the

non-targeted ones.

9. Visualizing Adversarial Noise

We visualize the amount of noise added to several examples in Figure 5 and 6. As shown, in each example, the noise is added to a region of image corresponding to the selected object

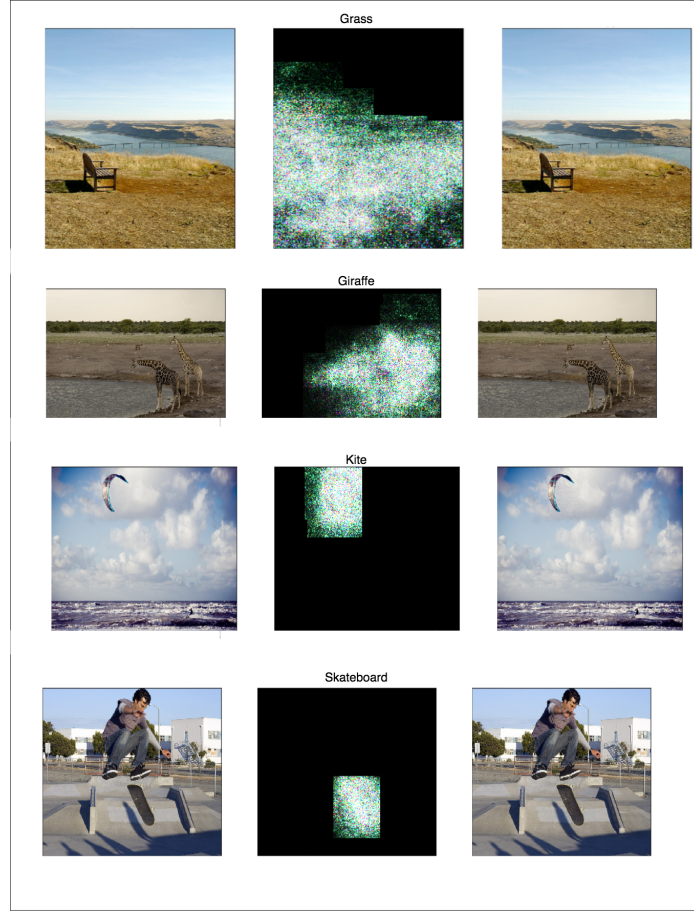


Fig. 5. Each row contains the original image, adversarial perturbation and the adversarial image (from left to right). The first two rows are from TAR-FREQUENT and the last two rows are from TAR-CONFIDENT. We show o_{pick} on top of each row. “grass” changes to “star” and “giraffe” changes to “lion” in the first and second rows, respectively. “kite” changes to “eyes” and “skateboard” changes to “column” for the third and fourth rows, respectively.

Table 8. Examples of predicted captions for adversarial and original image using different attack approaches.

APPROACHES	ORIGINAL CAPTIONS	ADVERSARIAL CAPTIONS
DAG	Two stuffed teddy bears sitting on a bed. A man riding a horse in front of a crowd. A person holding a hot dog on a bun.	A blender that is sitting in the water. A bunch of food on a grill with meat being dogs. A close up view of an airplane with a knife.
TAR-FREQUENT	A donut and a donut sitting on a table. A man jumping a skateboard on a skateboard. Two birds are flying over a building in a city.	A plate with a doughnut and a donut on it. A man jumping through the air with a skateboard. Two birds sitting on a boat in the water.
TAR-CONFIDENT	A man riding a horse in front of a crowd. A black and white photo of a city street with cars. A living room with a table and a table.	A person riding a horse in front of a dog. A tower with a clock on top of it. A man taking a picture in a bathroom mirror.
NON-TAR-FREQUENT	Two cats sitting in a bath tub sink. A black and white photo of a city street with cars. A living room with a table and a table.	A black and white dog is standing in a boat. A black and white photo of a city street with cars. A living room with a couch and a table.
NON-TAR-CONFIDENT	A group of people walking around a parking meter. A television and a television in a room. A vase with white flowers on a desk.	A man is holding a parking meter on a pole. A living room with a couch and a chair. A vase with white flowers on a desk.

(o_{pick}). We did this by defining M (our binary mask) in Equation 2. For example, the sample objects of “grass” and “giraffe” are chosen and attacked in the first two rows of Figure 5 by TAR-FREQUENT. These objects are the most frequent objects in the corresponding images and their corresponding masks are big-

ger than the last two rows in the figure. They are also successfully changed to “star” and “lion”, respectively. In the last two rows, the sample objects of “kite” and “skateboard” (the most confident objects) are attacked in the images by TAR-CONFIDENT. They are changed to “eyes” and “column”, respectively. In ad-



Fig. 6. Each row contains the original image, adversarial perturbation and the adversarial image (from left to right). The first two rows are from NON-TAR-FREQUENT and the last two rows are from NON-TAR-CONFIDENT. We show o_{pick} on top of each row. For example, “tie” is o_{pick} in the first row.

dition, we have also shown some samples of our non-targeted attacks in Figure 6. For example, the sample objects of “tie” and “bench” are attacked in the first two rows of the figure by NON-TAR-FREQUENT. These are the most frequent objects in the images. In the last two rows, “whiskers” and “light” are attacked by NON-TAR-CONFIDENT. These are the most confident objects in the images. In these non-targeted attacks, we do not target any specific class and the most frequent objects usually come with bigger masks compared to the most confident ones.

10. Captions

Table 8 shows examples of predicted captions for adversarial and original images using different variants of PICK-OBJECT-ATTACK and DAG. As we can see DAG leads to image captions which are entirely unrelated with the original captions such as “A man riding a horse in front of a crowd” becomes “A bunch of food on a grill with meat being dogs”.

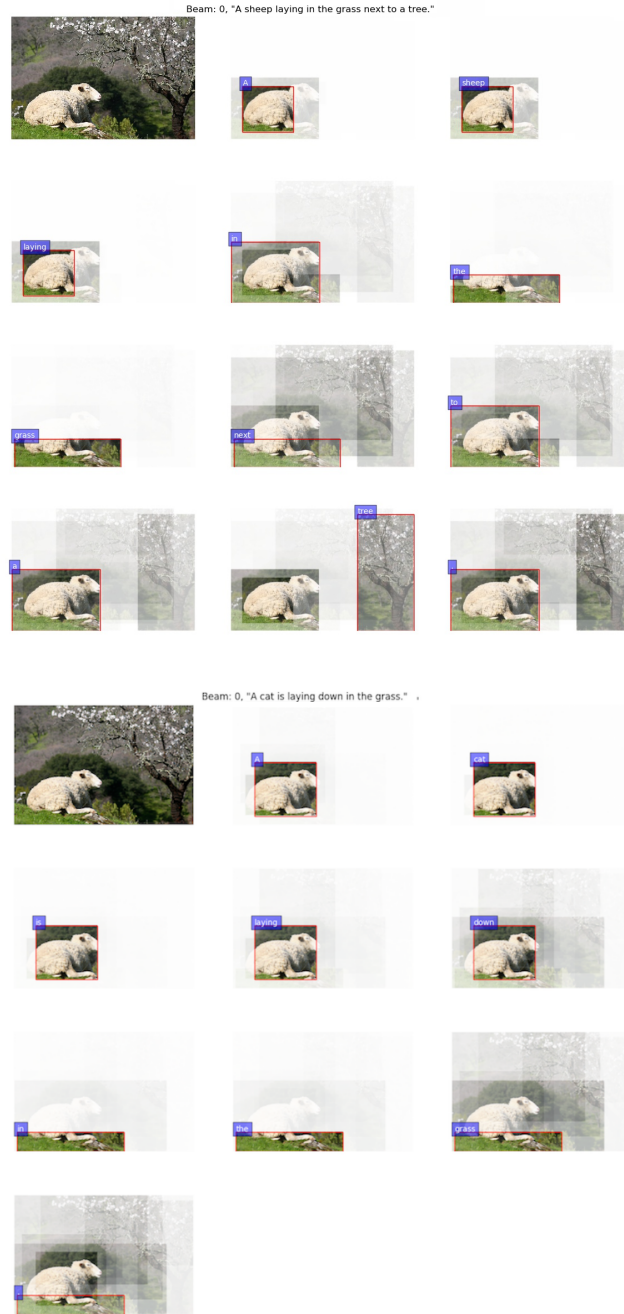


Fig. 7. The attention visualization for the caption of the original image (the top image) and the adversarial image (the bottom image). The adversarial image was obtained by TAR-CONFIDENT and the original class was “sheep” (o_{pick}). In this example, the caption of the adversarial image includes the targeted class, “cat” (k).

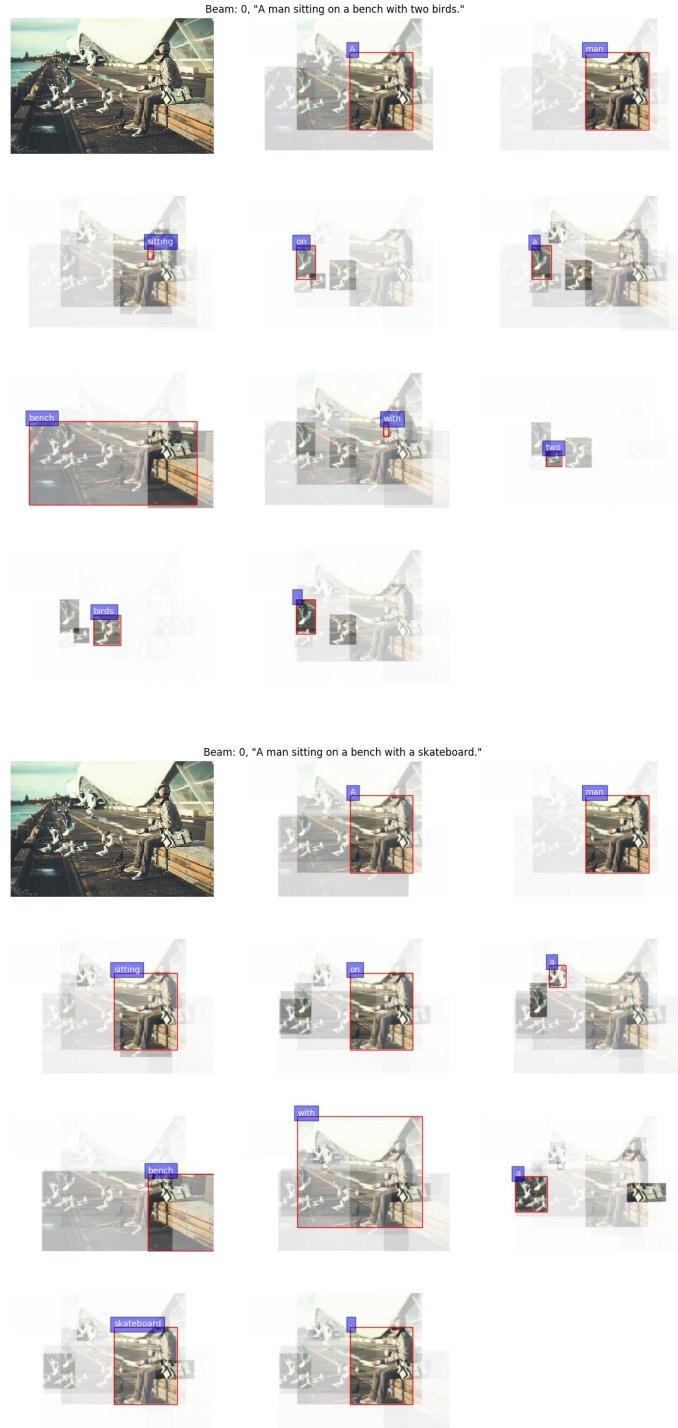


Fig. 8. The attention visualization for the caption of the original image (the top image) and the adversarial image (the bottom image). The adversarial image was obtained by TAR-FREQUENT and the original class was “bird” (o_{pick}). In this example, the caption of the adversarial image does not include the targeted class, “sign” (k).